VOL. 13, NO. 24, DECEMBER 2018 ISSN 1819-6608
ARPN Journal of Engineering and Applied Sciences

www.arpnjournals.com

CONTRIBUTION OF GEOSTATISTICAL ANALYSIS FOR THE ASSESSMENT OF RMR AND GEOMECHANICAL PARAMETERS

Amine Soufi, Lahcen Bahi and Latifa Ouadif
Laboratory of Applied Geophysics, Geotechnics, Engineering Geology and the Environment
Civil Engineering, Water, Environment and Geosciences Center, Morocco
Mohammadia School of Engineers, Mohammed V University, Rabat, Morocco
Email: amine.soufi@outlook.com

ABSTRACT

Geotechnical and engineering geology practitioners are always looking out for tools which can help understand and reduce the large uncertainty and variations in rock masses after complex geological processes. Relying on traditional interpolation techniques for geotechnical variables may lead to large uncertainty and major stability risk in the mining phase. The present paper proposes a direct and indirect methodology based on geostatistical estimation and simulation techniques to determine the expected Rock Mass Rating (RMR) and its underlying parameters, each geostatistical model identifies potential risk-prone areas in which failures could be experienced, superposing the different resulting maps allowed us to define low-risk conservative RMR model. A total of 115 underground rock blocks samples from five mining openings were examined for the rock mass quality using the RMR, Q and RMi characterization systems. Cross-validation and jack-knifing techniques showed that the proposed indirect estimation and simulation methods outperformed the more frequently used direct approach and shows a more accurate map with a low error coefficient which makes them adequate for RMR modeling. The resulting map of the indirect approach allowed taking into account the nonlinear nature, directional behavior of the RMR and its constitutive parameters which can be used to assist engineers in proposing suitable excavation techniques and an appropriate support system. The developed model help to assess different geomechanical parameters that can use to develop numerical models that explicitly consider the rock mass heterogeneity.

Keywords: geomechanics, rock mass rating, geostatistical analysis.

List of symbols or abbreviations

OK :	Ordinary kriging
SK :	Simple kriging
OK_i	Indirect ordinary kriging
OK_d	Direct ordinary kriging
OCK :	Ordinary co-kriging
OCK1 :	Ordinary co-kriging (Q* as a covariate)
OCK2 :	Ordinary co-kriging (RMi* as a covariate)
CGS :	Conditional Gaussian simulation
GCS_i	Indirect Gaussian conditional simulation
GCS_d	Direct Gaussian conditional simulation
IDW :	Inverse distance weighting
v :	Spherical variogram model
Exp :	Exponential variogram model
Gaus :	Gaussian variogram model
L_s :	Variogram Lag size
C_0 :	Nugguet semivariance
C_{00} :	Nugget semivariance of the Primary variable
C_{11} :	Cross-variogram Nugget semivariance
$Sill_{00}$:	The sill of the primary variable variogram
$Sill_{01}$:	The sill of the covariate variogram
$Sill_{11}$:	Cross-variogram sill
RMR :	Rock mass rating
RMi :	Rock mass index
Q :	Rock mass quality
UCS :	Uniaxial compressive strength
RQD :	Rock quality designation
Jn :	Joint set number
Jr :	Joint roughness number
Ja :	Joint alteration number
Jw :	Joint water reduction factor
Jc :	Joint surface condition
RSS :	Residual sum of squares
RMSE :	Root mean squared error
MAPE :	Mean absolute percent error
NMAE :	Normalized mean-absolute error
S_k :	Skewness
K_r :	Kurtosis
GSI :	Geological strength index
E_m :	Rock mass deformation modulus
σ_{cm} :	Rock mass compressive strength
φ_m :	Internal friction angle of rock mass
c_m :	The cohesion of rock mass
r^2 :	Coefficient of determination
Q^*:	Q-system transformed covariate variable
RMi^*:	RMi transformed covariate variable
p	IDW exponent value
$\gamma^*(h)$	Experimental Semivariogram
Min	Minimum value
Max	Maximum value

1. INTRODUCTION

Geotechnical engineering practitioners are always looking out for tools which can improve the design and help understand and reduce the large uncertainty and variations in rock masses. In the literature, only a few applications can be found aiming the estimation of RMR (Ferrari *et al*, 2014) [1] (Marisa Pinheiro *et al*, 2016) [2] (Hesameddin Eivazy, 2017) [3]. These authors have concluded that rock mass parameters are reasonably predictable in unsampled locations using geostatistical interpolation methods. These analyses have been applied to specific geotechnical problems on limited area and localized sites.

Rock masses are characterized by uncertainty and heterogeneity after complex geological processes. Relyingon traditional interpolation methods may lead to large uncertainty and major stability risk in the mining phase. The tackling of the described problems can be made using a sophisticated analysis taking into account the spatial relationship of a modeled the rock mass rating which is a very significant criterion to evaluate the stability of an underground mining area.

Rock mass rating was developed by Bieniawski [4], it is an index of rock mass competency based on the rating of five parameters:

A_1	Intact rock strength
A_2	Rock quality designation (RQD)
A_3	Joint spacing (Js)
A_4	Joint surface condition (Jc)
A_5	Groundwater condition (Jw)

$$RMR_{basic} = \sum_{i=1}^{5} A_i \quad (1)$$

This paper focuses on applying and comparing different geostatistical techniques to predict basic RMR values, directly and indirectly, performs quantifying uncertainty prediction taking into account spatial variability**.** The analysis is made in an attempt to use these interpolations for assessment of rock mass geomechanical parameters.

The interpolation results obtained by direct and indirect approach are statistically compared via cross-validation and jack-knifing techniques in order to measure the benefits of using geostatistics.

2. GEOLOGICAL SETTING AND CASE STUDY

Imiter silver mine is located on the northern side of the Precambrian JbelSaghro inlier (eastern Anti-Atlas, Morocco) (Figure-1), north of the West African Craton. Two major lithostructural units are recognized: the lower complex made of Middle Neoproterozoic detrital sediments intruded by ca. 570–580 Ma diorite and granodiorite plutons, the upper complex composed by lava flows and ash-flow tuffs associated with cogenetic granites. The Imiter deposit, localized along N070–090° E-trending regional faults system is assumed to be a Late Neoproterozoic epithermal deposit, hosted by both lower and upper complexes. The ore deposition is genetically associated with the felsic volcanic event, dated at 550 Ma, and assumed to result from a regional extensional tectonic regime.

The Imiter fault system, 10-km long, is localized at the contact between lower and upper complexes (Figure-1b). It consists in the association between N090°E and N060–070 °E faults that define a succession of apparent left-lateral pull-apart texture, at map scale (Figure-1). At Imiter II, the main B3 corps (sampling area) is oriented N065 °E with a south dipping and intercepted by four sets of discontinuities (Figure-3).

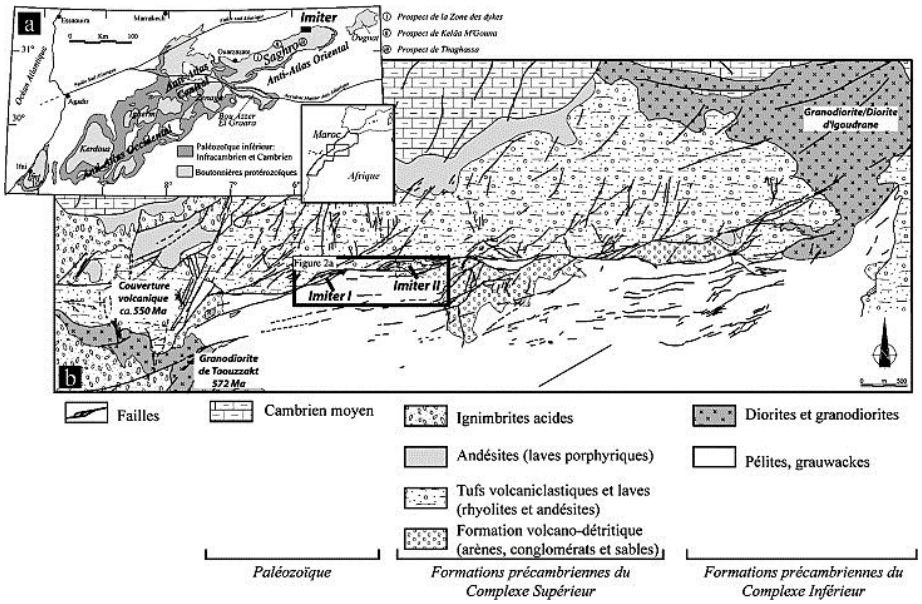

Figure-1. a) Schematic map of the Moroccan Anti-Atlas and localization of the Imiter silver mine and other mineral bearing indices of the JbelSaghro. (b) Simplified geological map of the Imiter silver mine.

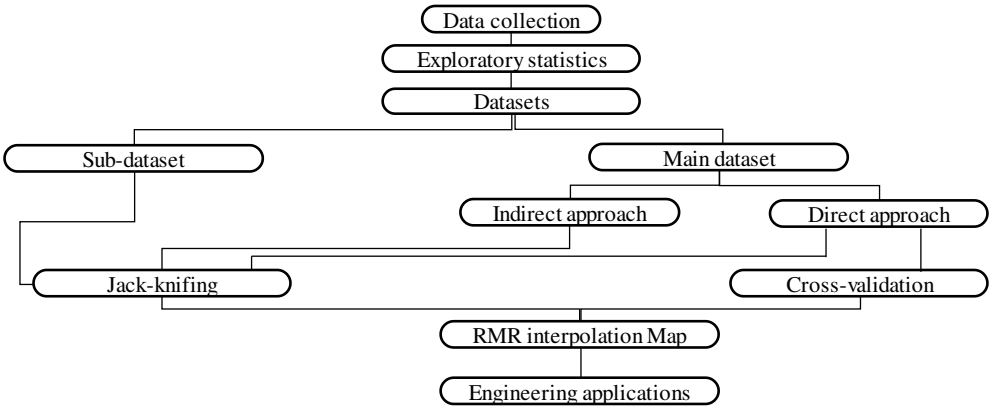

Figure-2. Flowchart of the research approach.

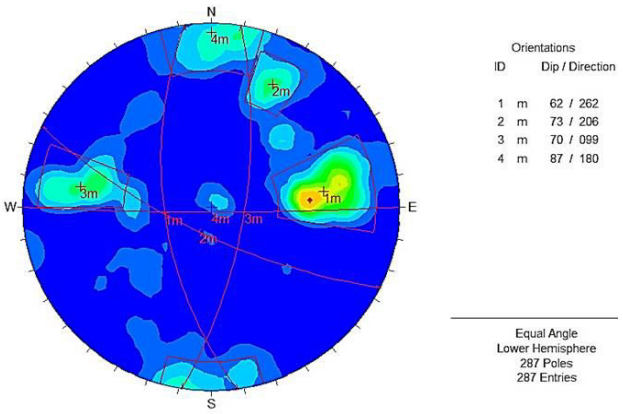

Figure-3. Stereonet diagram (lower hemisphere) showing the main discontinuities sets of the sampling zone.

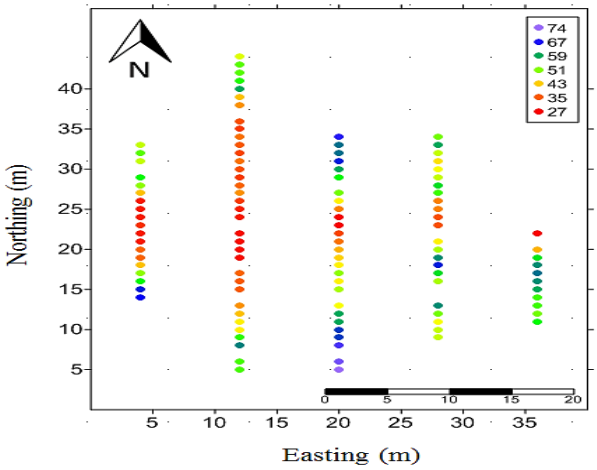

Figure-4. Map of spatial distribution for basic RMR values.

The study area is at a depth of 500m is characterized by:

- The common rock type are meta-siltstones
- There are prominent foliations over all the rock mass in Est-West direction.
- There are multiple discontinuity sets, many of which intersect each other.

The underground geotechnical surveys method provides a great opportunity for engineers and geologists to observe and sample the rock mass on the excavation faces. A total of 115 rock blocks samples from five mining openings were examined for the rock mass quality using the RMR (Figure-4), Rock Quality system (Q) and Rock Mass Index (RMi) characterization systems, the outcrop mapping was carried out on freshly exposed parallel faces in the horizontal south to north direction to simplify variables with directional behavior.

3. EXPLORATORY STATISTICAL ANALYSIS

To provide an overview of the measured selected variables data, a basic statistical study was made. Classical descriptors were determined, such as mean, maximum, minimum, standard deviation and skewness (S_k) of data distribution.

The descriptive statistics of the rock mass rating data suggested that the RMR may vary from 27 to 74 with a mean value of 46.9% and standard deviation of 11,72%, the geomechanical quality of the rock mass varies from poor to good. The summary of the statistics for rating parameters is shown in (Table-1).

The coefficients of variation of RMR parameters ranged from 7% to 43%, It was noted the presence of a strong spatial variability of RMi and Q ratings with a variation coefficient of 103% and 154% respectively.

Once the data set was checked, the next step was generating the histogram to study the symmetry and pattern of the frequency distribution and to determine how much percent of the samples are far from the central value. The histogram of RMR, RMi and Q values are displayed in (Figure-5).

The uniaxial compressive strength (UCS), Q, and RMi data were positively skewed, the rest of other parameters

Table-1. Descriptive statistics of rock mass collected data.

		Max	Min	Standard deviation	Median	Average	Variance	Skewness	Kurtosis
Ratings	UCS	4.91	3.63	0.29	3.76	3.87	0.08	1.40	1.49
	RQD	20.00	5.00	4.36	8.00	9.72	19.00	0.41	-1.16
	Js	10.00	5.00	1.70	8.00	7.32	2.88	-0.25	-1.07
	Jc	28.00	2.00	5.55	12.00	13.04	30.77	0.33	-0.45
	Jw	15.00	9.00	2.48	15.00	12.94	6.16	-0.38	-1.87
	RMR	74.91	27.63	11.72	47.78	46.90	137.4	0.08	-0.92

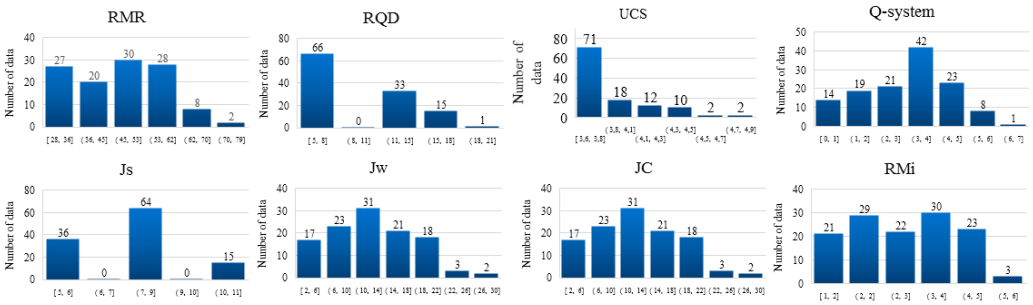

Figure-5. Frequency distribution for modelling variables.

were normally distributed (skewness of between -1 and 1), there are some maxima, but the entire distribution can be treated as having a single peak.

4. TREND ANALYSIS

Many geostatistics techniques assume of spatial stationarily, the validity of this property (i.e. The absence of regular trends in space) needs to be verified by projecting the sample locations on an x, y plane. The RMR value of each sample is given in the z dimension (Figure-6).

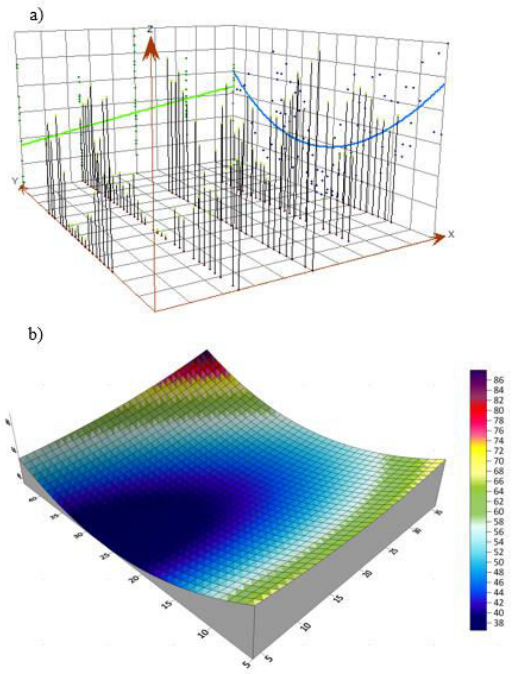

Figure-6. RMR trend analysis projections.

The Trend Analysis of RMR data does not present any systematic trend or change in space, because the values cannot be interpolated by a monotone ascending or descending function in the studied domain, this leads to assume a ‘‘trend’’ free case in this study where stationarily condition can be applied and kriging can be allowed.

5. MODEL EVALUATION

The evaluation of RMR variograms and maps accuracy is based on the following parameters:

- The root-mean-square error (RMSE) :

$$RMSE = \sqrt{\frac{1}{n}\sum_{i=1}^{n}(A_t - F_t)^2} \quad (2)$$

- The Residual sum of squares (RSS) :

$$RSS = \sum_{i=1}^{n}(A_t - F_t)^2 \quad (3)$$

- The normalized mean-absolute error (NMAE) :

$$NMAE = 100\% \sum_{i=1}^{n}\frac{A_t - F_t}{A_t} \quad (4)$$

- The mean absolute percentage error (MAPE) :

$$MAPE = \frac{1}{n}\sum_{i=1}^{n}\left|\frac{A_t - F_t}{A_t}\right| \quad (5)$$

Where, A_t Is the actual value, F_t Is the predicted value of the output variable and n is the number of samples.

6. SPATIAL ANALYSIS

6.1. Geostatistical estimation

McDonnell & Burrough (1998) [5] have shown that for applications in geosciences, Kriging is the best linear unbiased estimator (Journel and Huijbregts, 1978) [6] (Isaaks and Srivastava, 1989) [7]. The construction of the kriging estimator is done by successively imposing these features (linearity, unbiasedness, optimality). Variations of the estimate are achieved by imposing a known or unknown mean and allowing local variations of it (Goovaerts, 1997) [8].

6.2 Geostatistical simulation

Geostatistical simulation is a stochastic, nonlinear modeling method that obtains multiple plausible realizations of spatial variability based on the same input data according to the following criteria (Dowd, 1993) [9]:

- At all sampled locations they honor the real values,
- They have the same spatial dispersion (i.e. same variogram, as the true values),
- They have the same distribution as the true values

6.3 Variography analysis

Spherical, exponential and Gaussian isotropic theoretical functions were fitted to the sample variograms depending on the shape using a weighted least squares method (Robertson, 1987) [10] procedure and cross-validation technique. 0The parameters of the model: nugget semivariance, range, and sill or total semivariance were determined.

To define different classes of spatial dependence for RMR, the ratio between the nugget semivariance and the sill was used (Cambardella *et al,* 1994) [11]. If the ratio was ≤25%, the variable was considered to be strongly spatially dependent, or strongly distributed in patches, the RMR was considered strongly spatially dependent.

7. DIRECT APPROACH

In the direct approach, the RMR basic values were used directly as inputs to inverse Distance Weighting, geostatistical estimation, and simulation in order to create 2D models of RMR in the mining area. This approach neglects the nonlinear nature of RMR underlying variables. However, it is considered as a simple, quick and practical solution.

7.1 Inverse distance weighting

Inverse Distance Weighting (IDW) interpolation is a deterministic, nonlinear interpolation technique that uses a weighted average of the attribute values from nearby sample points to estimate the magnitude of that attribute at non-sampled locations, assuming that each measured point has a local influence that diminishes with distance. It weights the points closer to the prediction location greater than those farther away. IDW is calculated as:

$$Z^*(u) = \sum_{i=1}^{n} \lambda_i Z(u_i) \quad (6)$$

$Z(u_i)$ Are the conditioning data
n is the number of sample points
λ_i Are the assigned weights
The weights are determined as:

$$\lambda_i = \frac{\frac{1}{d_i^p}}{\sum_{i=1}^{n} \frac{1}{d_i^p}} \quad (7)$$

$$\sum_{i=1}^{n} \lambda_i = 1 \quad (8)$$

d_i Are the Euclidian distances between estimation location and sample points
p is the power or distance exponent value.

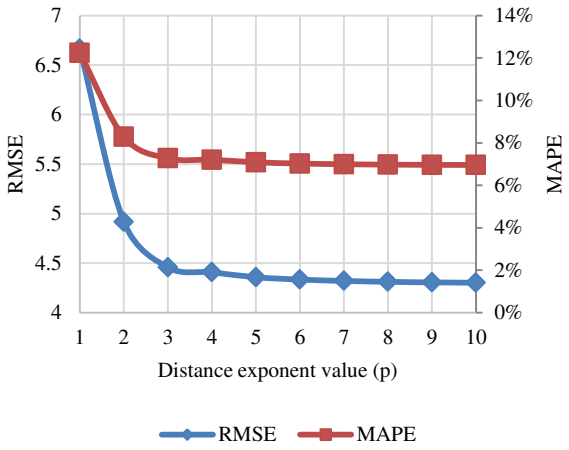

Figure-7. RMSE and MAPE plotted for several different powers.

The optimal power value is determined by minimizing the root mean square error and the mean absolute percentage error calculated from RMR cross-validation.

Figure-7 shows that IDW with power 10 is an optimal distance exponent value that produces the minimum RMSE and MAPE. As *p* increases only the immediate surrounding data points will influence the RMR prediction.

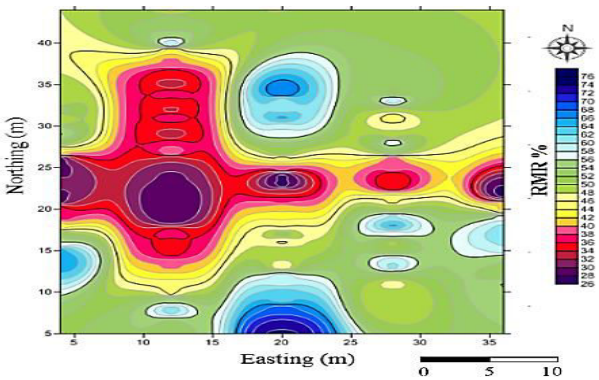

Figure-8. IDW interpolation map for RMR data.

Table-2. Results of OK variography analysis.

	Variogram parameters					Goodness-of-fit		Cross-validation
Models	L_s	C_0	Range	Sill	C_0/Sill %	RSS	R²	RMSE
Sph	1.41	0	11.35	139.15	0	794	0.958	3.912
Exp	2.76	0	22.12	170.53	0	310	0.995	4.38
Gaus	1.43	11.42	8	125.49	9	1742	0.964	4.505

7.2 Ordinary kriging

Ordinary kriging (OK) is the most widely used kriging method. It serves to estimate a value at a point of a region for which a variogram is known, using data in the neighborhood of the estimation location. The spatial distribution of the rock mass rating data was analyzed using geostatistics. Spatial patterns are usually described using the experimental Semivariogram $\gamma^*(h)$,which measures the average dissimilarity between RMR data separated by a vector h.

$$\gamma^*(h) = \frac{1}{2N(h)}\sum_{i=1}^{n(h)}[z(x_i) - z(x_i + h)]^2 \quad (9)$$

where n is the number of pairs of sample points separated by the distance h.

Semivariogram sample is calculated from the data sample using the following equation:

$$Z^*(x) = \sum_{i=1}^{n}\lambda_i z(x_i) \quad (10)$$

$Z^*(x)$: prediction location

$$\sum_{i=1}^{n}\lambda_i = 1 \quad (11)$$

λ_i : unknown weight of measured value of pairs of point
$Z(x_i)$: measured value of pairs of point
n : number of measured values

The most important step in the use of geostatistical methods is to obtain the variogram with high correlation.

This step has a significant impact on the behavior and results of the model. Spherical, exponential, Gaussian models were fitted to the RMR empirical semivariograms assuming isotropic condition.

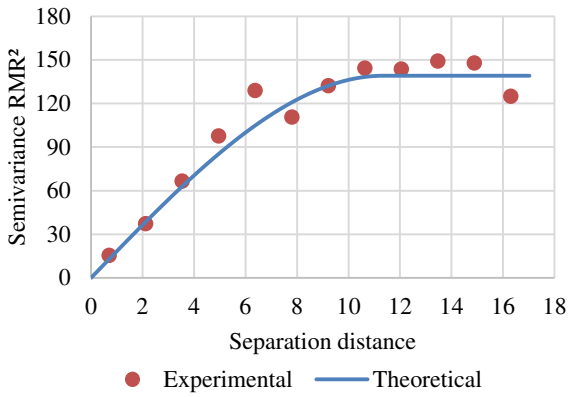

Figure-9. OK Experimental Semivariogram and fitted model for RMR data.

Figure-9 shows the empirical variogram, which is a plot of the values of as a function of h, gives information on the spatial dependency of the RMR variable. The Spherical model with the smallest RMSE=3.912 (Table-2) was selected to describe the RMR spatial dependency (Figure-10).

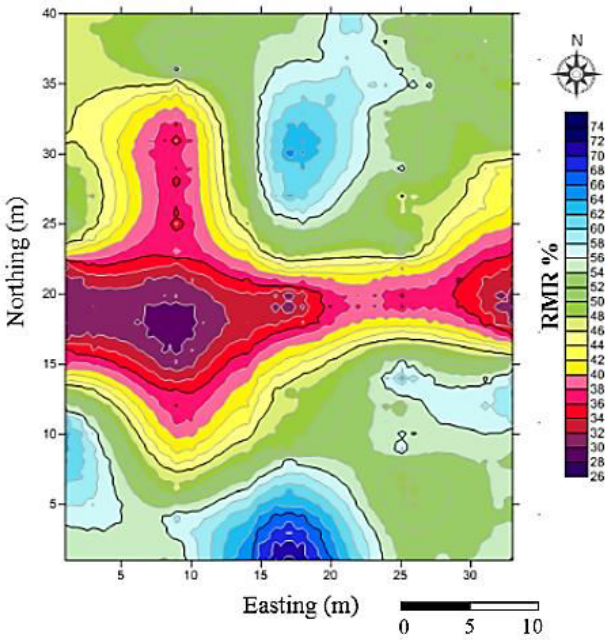

Figure-10. Ordinary kriging map for RMR data.

Table-3. Results of the RMR-Q* cross-variography analysis.

		Variogram parameters							Goodness-of-fit		Cross-validation
RMR x Q*	Models	L_s	C_{00}	C_{11}	Range	$Sill_{00}$	$Sill_{01}$	$Sill_{11}$	RSS_{11}	R^2_{11}	RMSE
	Sph	1.57	0.078	0.042	12.6	148.71	1.94	13.38	50.1	0.942	3.452
	Exp	2.5	0	0	20.03	166.35	2.37	10.25	6.35	0.967	3.443
	Gaus	1.49	10.93	0.137	7.97	124.58	1.7	13.88	15.1	0.986	4.223

Table-4. Results of the RMR-RMi* cross-variography analysis.

		Variogram parameters							Goodness-of-fit		Cross-validation
RMR x RMi*	Models	L_s	C_{00}	C_{11}	Range	$Sill_{00}$	$Sill_{01}$	$Sill_{11}$	RSS_{11}	R^2_{11}	RMSE
	Sph	1.49	0	0	11.99	145.62	1	10.51	46.8	0.929	4.506
	Exp	2.34	0	0	18.74	163.46	1.48	8.44	13	0.903	3.723
	Gaus	1	3.54	0.1	6.57	127.21	1.08	11.57	17.4	0.955	3.811

7.3 Ordinary cokriging

The ordinary cokriging (OCK) procedure is an extension of kriging when a multivariate variogram model and multivariate data are available. The spatial dependence between the RMR and Q-system or RMI was estimated by means of a cross-variogram given by the following equation (Deutsch and Journel, 1992) [12] (Yates and Warrick, 1987) [13]:

$$\gamma_{AB}{}^{*}(\mathrm{h}) = \frac{1}{2\mathrm{N(h)}}\sum_{\mathrm{i}}^{\mathrm{n}}\sum_{\mathrm{j}}^{\mathrm{m}}\{\mathrm{z_A(x_i)} - \mathrm{z_A(x_j)}\}\{\mathrm{z_B(x_i)} - \mathrm{z_B(x_j)}\} \quad (12)$$

$\gamma_{AB}{}^{*}(h)$: is the estimated cross-variogram value at distance h

$N(h)$ is the number of data pairs of observations of the first variable z_A and the second variable z_B at locations $x_i$and $x_j$when the distance between xi and xj fits in a distance class h.

The cokriging estimate is a linear combination of both the RMR and the secondary variables Q or RMi given by:

$$Z^{*}(x) = \sum_{i=1}^{n} w_i z(x_i) + \sum_{j=1}^{m}\sum_{i=1}^{n} v_{ij} u(x_{ij}) \quad (13)$$

Subject to one of the following sets of linear constraints:

$$\sum_{i=1}^{n} w_i + \sum_{j=1}^{m}\sum_{i=1}^{n} v_{ij} = 1 \quad (14)$$

Where, w_iAre the kriging weights associated with the n-nearest neighbors, v_{ii}, are the cokriging weights associated with the m auxiliary variables, u_{ij}That are spatially correlated to the variable of interest.

In the present study, we consider the following transformation for covariate variables:

$$Q^{*} = \ln(Q) + 3.5 \quad (15)$$

$$RMi^{*} = \ln(RMi) + 3.5 \quad (16)$$

Finding cokriging theoretical models that fit best the experimental Semivariogram (Figures 11, 12) and cross-variograms (Figure-13) with less error coefficient is, however, a difficult exercise. The selection was made on the basis of cross-validation parameter (RMSE) to assess the precision of the interpolation method (Tables 3, 4).

When models are fitted to the experimental semi- and cross-variograms, the Cauchy-Schwartz equation must be checked to guarantee a correct Cokriging estimation variance in all circumstances (Deutsch and Journel 1992) (Isaaks and Srivastava 1989)

$$\left|\gamma_{RMR-Q}\right| \leq \sqrt{\gamma_{RMR} \cdot \gamma_{Q}} \quad (17)$$

γ_{RMR-Q} is the cross-variogram value
γ_{RMR} is Semivariogram value of RMR
γ_{Q} is Semivariogram value of Q-system

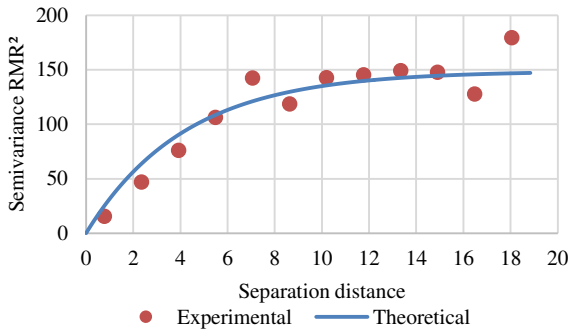

Figure-11. OCK Experimental Semivariogram and fitted model for RMR data.

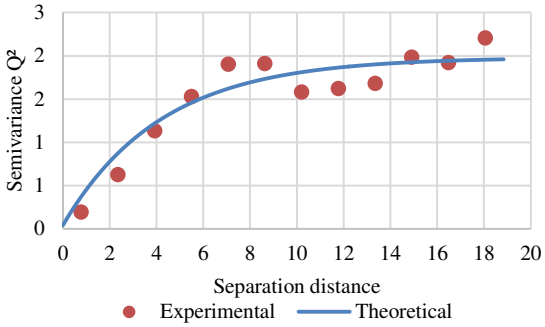

Figure-12. OCK Experimental Semivariogram and fitted model for Q* data.

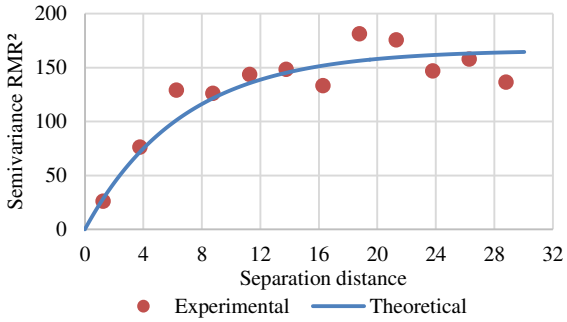

Figure-13. OCK Experimental and fitted cross-Semivariogram

After evaluating different models, it was demonstrated that the exponential model best suited for both variables RMR and Q with the lowest RMSE= 3,443 (Table-3) and therefore, it was selected as a best-fitted model for cokriging map (Figure-14).

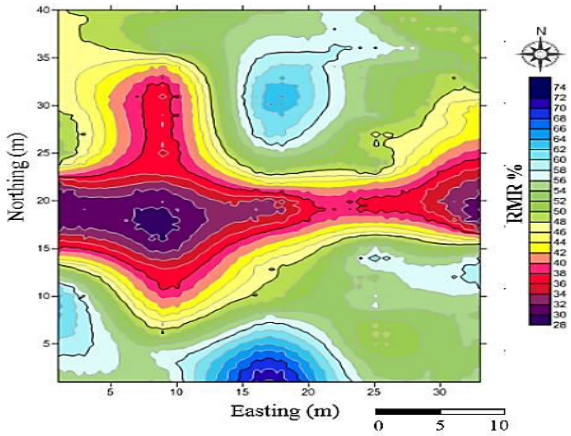

Figure-14. Ordinary cokriging map for RMR data.

7.4 Sequential Gaussian simulation

In this paper, geostatistical simulation is used in order to give an advantage to spatial correlation of RMR data; Sequential Gaussian simulation is the most commonly used method to develop conditional simulations.

This method requires a Gaussian transformation of the original RMR data set, to accomplish this, the RMR sample data were normalized using the two steps Approach for Transforming Continuous Variables to Normal was conducted (Templeton, 2011) [14], histograms, box-plot Q-Q plot was graphical ways to judge whether RMR transformed data are normally distributed (Figures 15, 16).

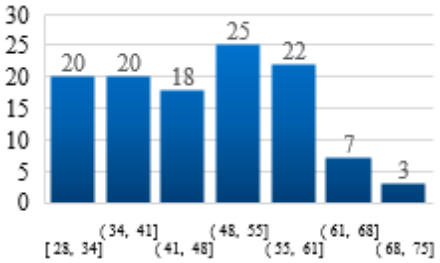

Figure-15. Histogram of RMR original data.

Table-5. Results of simple kriging variography analysis.

	Variogram parameters					Goodness-of-fit		Cross-validation
Models	L_s	C_0	**Range**	**Sill**	C_0/Sill %	**RSS**	**R²**	**RMSE**
Sph	1.35	0	10.86	138.49	0	323	0.982	4.374
Exp	2.4	0	19.27	160.53	0	537	0.975	4.495
Gaus	1	16.3	8.22	140.8	11.5	807	0.959	4.418

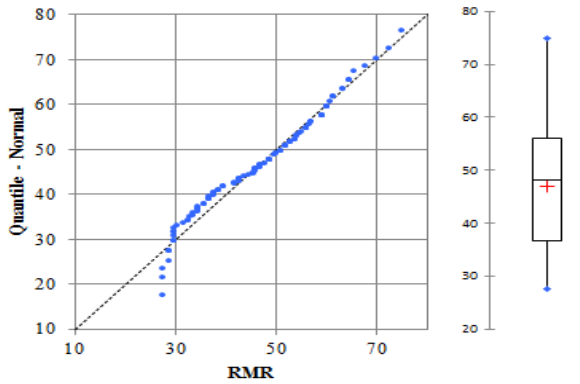

Figure-16. Q-Q and box plots of RMR original data.

The RMR datain (Figure-15) showsa left-skewed histogram has a peak to the right of center, more gradually tapering to the left side. In (Figure-16), the left and right end of pattern are below and above the line y=x respectively, this departure from linearity described by a long tails at both ends of the data distribution

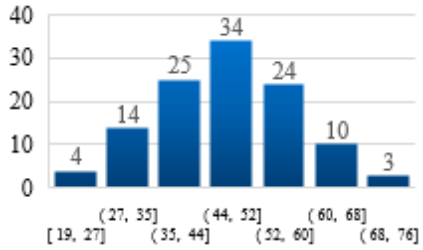

Figure-17. Histogram of RMR transformed data.

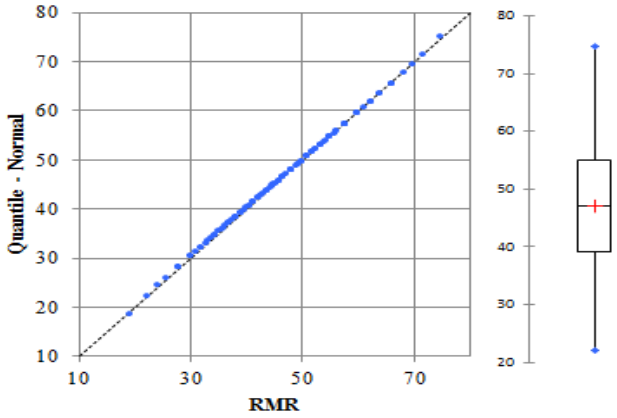

Figure-18. Q-Q and box plots of transformed RMR

Table-6. Normality parameters of RMR data.

RMR	Kurtosis	Skewness	Shapiro-Wilk
Original data	-0.916	0.077	0.007
Transformed data	-0.302	-0.001	0.998

In order to produce a conditional simulation, a new variogram must be developed with the Gaussian distribution then fitted (Figure-19) and cross-validated (Table-5), Variogram development, and simulations are performed on Gaussian transformed data and results must be back-transformed.

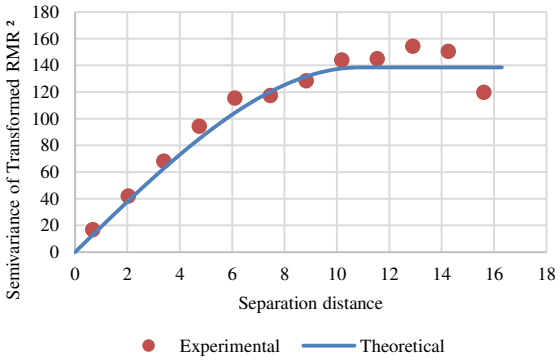

Figure-19. Simple Kriging Experimental Semivariogram and fitted model for RMR transformed data.

The results of conditional simulation are expressed by a number of equally probable maps, each realization obtained by using the conditional simulation method is equally valid, in this research, the number of RMR realizations is set to one thousand, so that the post-processing outputs (mean of the realizations and conditional probabilities) could be calculated with a reasonable approximation (Figure-20).

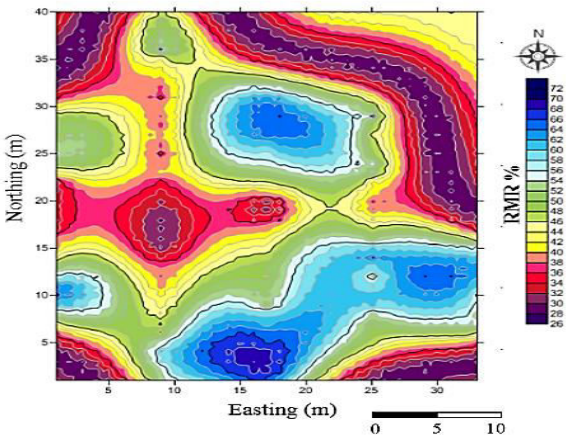

Figure-20. Conditional simulation map for back transformed RMR data.

A major limitation to the previous kriging methods that minimize the variance, inherently underestimates the variability and smooth out local details of RMR spatial variation, this can be a problem when trying to map sharp spatial poor-quality zones, therefore, conditional simulation is a robust way to create RMR exceedance probability maps (Figure-21).

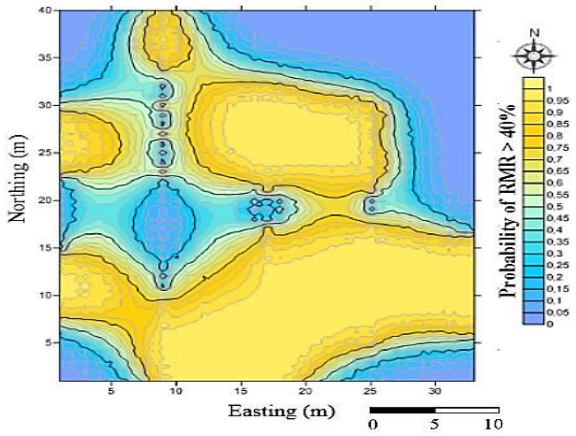

Figure-21. Exceedance probability map of RMR>40%.

8. INDIRECT APPROACH

RMR is a sum of ratings assigned non-linearly to several geotechnical parameters; the direct use of geostatistical techniques to estimate RMR does not account for the non-linearity property and may carry some estimation errors. However, each of the underlying components is an additive variable and therefore, can be directly averaged and modeled separately.

The indirect approach to spatial prediction, in this case, would be the following:

- Gaussian transformation of each RMR parameter R_i for conditional simulation, (Table-7)
- Variography analysis for OK (Table-8) and Simple kriging (SK) (Table-9)

Table-7. Normality coefficients of RMR parameters.

	RQD		UCS		Js		Jc		Jw	
RMR	S_k	K_t	S_k	K_t	S_k	K_t	S_k	K_t	S_k	K_t
Original data	0.408	-1.163	1.399	1.495	-0.253	-1.073	0.328	-0.448	-0.381	-1.868
Transformed data	0.265	-1.069	0.028	-0.311	0.255	-0.536	0.136	-0.108	-0.381	-0.582

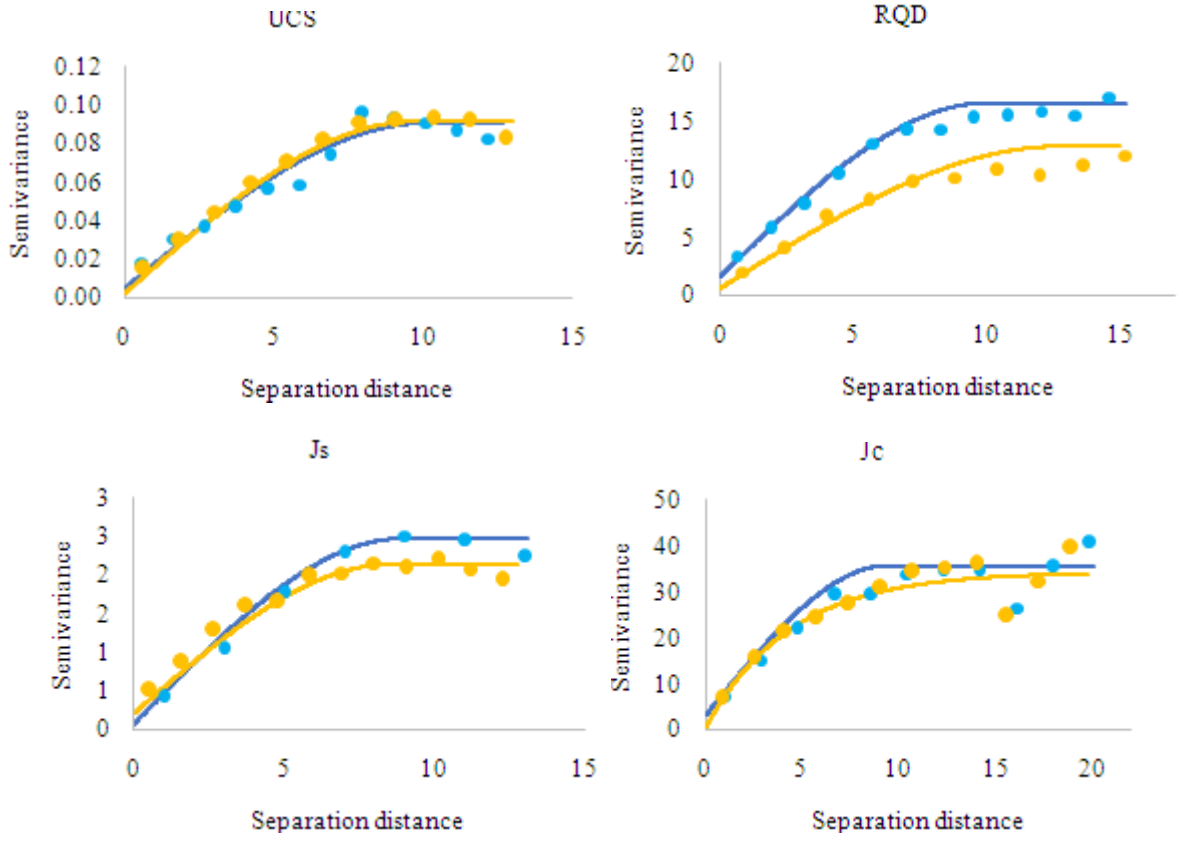

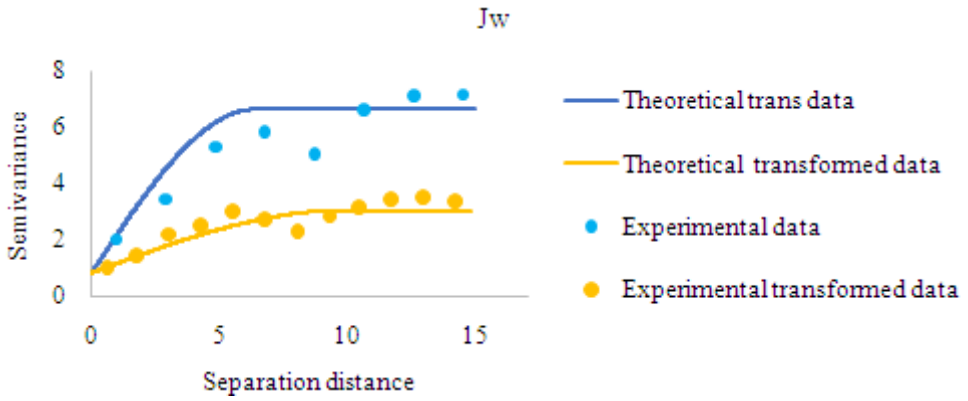

Figure-22. SK and OK Experimental Semivariograms and fitted models for rating data.

- Estimate and simulate each of RMR parameters which are linear variables (Figure-22)
- Assign a rating to the estimated or simulated value of each parameter.
- Back transformation of each simulated parameter R_i
- Obtain the final estimated (Figure-23) and simulated (Figure-24) rating RMR, as the sum of the ratings obtained

Table-8. Results of the indirect ordinary krigingvariography analysis for estimation.

R_i	Variogram parameters					
	Mod	L_s	C_0	Range	Sill	C_0/Sill
RQD	Spherical	1.26	1.6	10.02	15.89	10%
UCS		1.05	0.005	10.16	0.086	6%
J_S		2.98	0.001	8.42	2.48	0%
J_C		1.89	3.17	9.46	32.52	10%
W_i		1.93	0.78	6.38	5.85	13%

Table-9. Results of indirect simple kriging variography analysis for simulation.

R_i	Variogram parameters					
	Mod	L_s	C_0	Range	Sill	C_0/Sill
RQD	Sph	1.59	0.61	12.74	12.24	5%
UCS	Sph	1.21	0.002	9.72	0.089	2%
J_S	Sph	1.06	0.208	8.52	1.93	11%
J_C	Exp	1.64	0.51	13.17	33.77	2%
W_i	Sph	1.23	0.81	9.89	2.23	36%

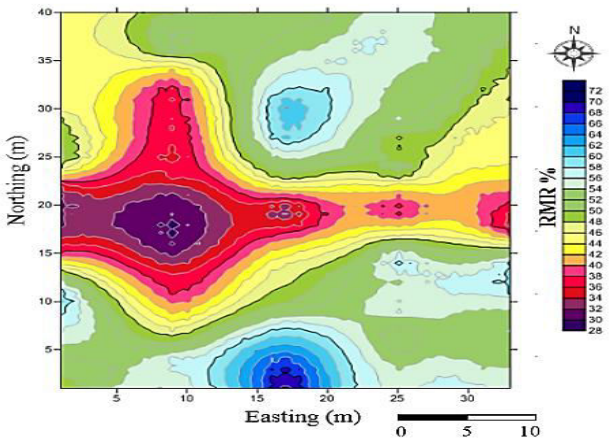

Figure-23. Indirect OK map for RMR data.

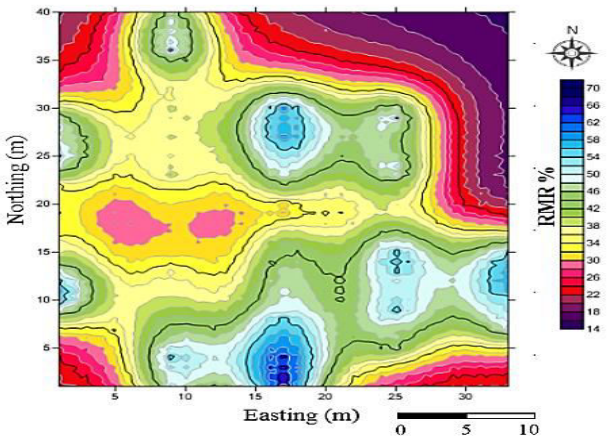

Figure-24. Indirect conditional simulation map for RMR data.

9. VALIDATION

9.1 Cross-validation

Several authors recommend the cross-validation technique for evaluating the accuracy of an interpolation technique (Webster and Oliver, 2001) [15] (Kravchenko and Bullock, 1999) [16]. Cross-validation is a leave-one-out technique that uses all of RMR data to estimate the autocorrelation models by removing data from 115

locations, taken all of the available data from other locations and then estimating the value of the removed locations data using those remaining data(Olea, 1999) [17].

In cross-validationanalysis, a graph can be constructed between the estimated and actual values for each sample location in the domain.

The cross-correlation plots showed that ordinary cokriging with the transformed Q covariate outperforms other direct predictions (Figure-27).

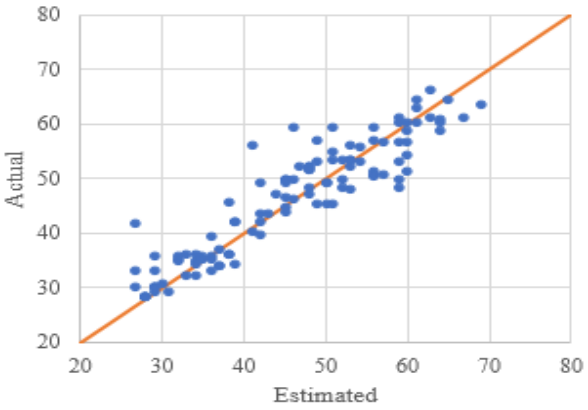

Figure-25. Scatter plots of IDW cross-validation results.

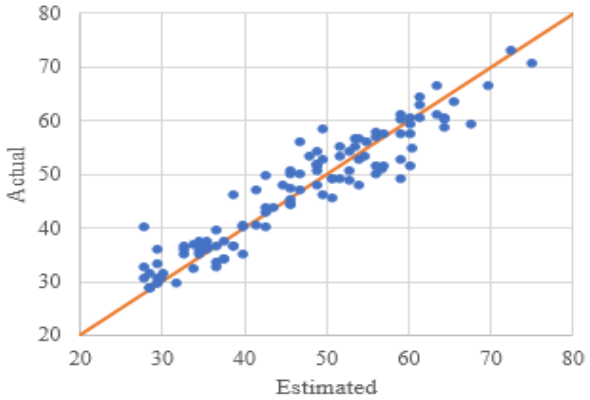

Figure-26. Scatter plots of direct OK cross-validation results.

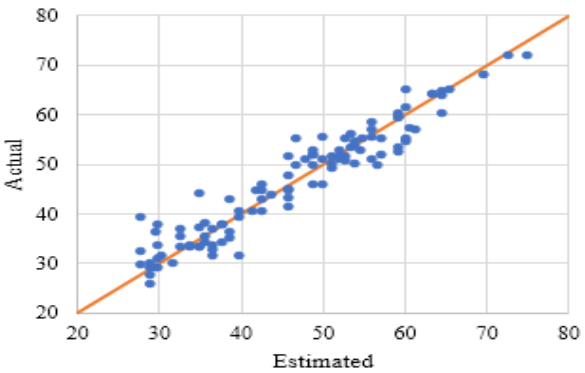

Figure-27. Scatter plots of OCK (RMR-Q*) cross-validation results.

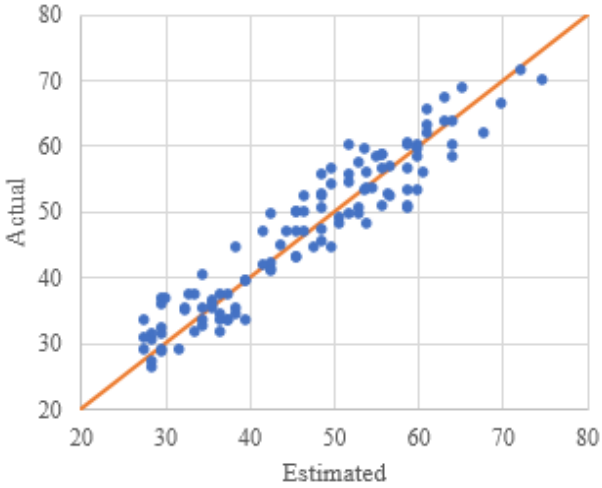

Figure-28. Scatter plots of OCK (RMR-RMi*) cross-validation results.

For all points, cross-validation compares the measured and predicted values. In this research, RMSE, MAPE, and NMAE are used to evaluate predicted value with IDW, okd,and OCK and helps us for determination the best RMR model.

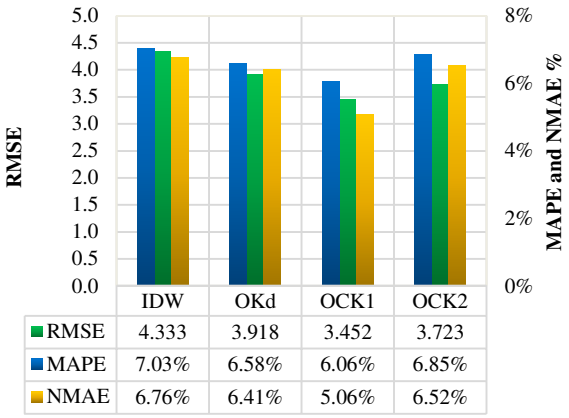

	IDW	OKd	OCK1	OCK2
RMSE	4.333	3.918	3.452	3.723
MAPE	7.03%	6.58%	6.06%	6.85%
NMAE	6.76%	6.41%	5.06%	6.52%

Figure-29. Error coefficients of cross-validation results.

The overall performance of RMR co-kriging with the transformed Q covariate was outstanding with exponential semi-variogram which gave the lowest error coefficients in all the cases (Figure-29).

9.2 Jack-knifing validation

With the aim of comparing results and selecting the most suitable interpolation technique out of above mentioned seven different methods, the jack-knifing process has been performed, using new samples. An independent data set of 13 RMR surveys have been carried out in the research area to be compared with the estimated data point (Figure-30).

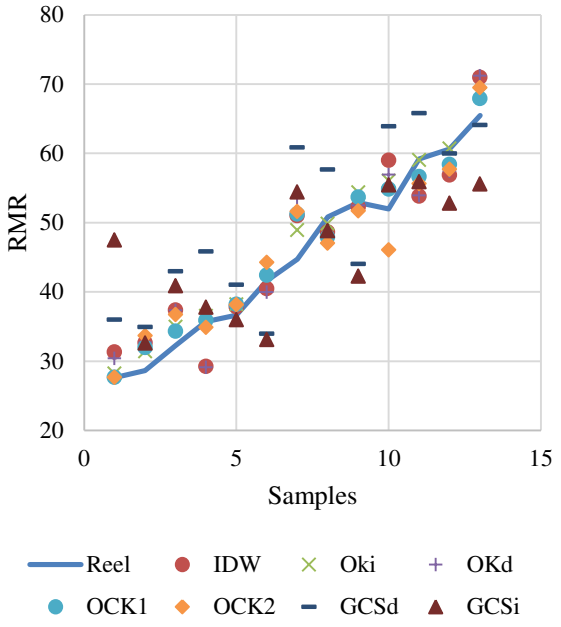

Figure-30. Scatter plots between RMR true values and interpolated results.

The RMSE, MAPE, and NMAE were employed as criteria to evaluate the accuracy and effectiveness of RMR prediction maps via jack-knifing data points.

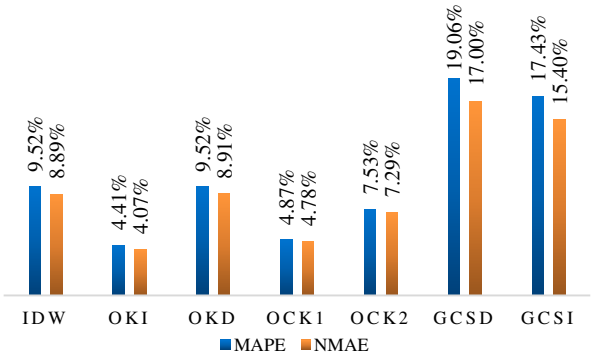

Figure-31. Error coefficients of jack-knifing data.

Comparingthe predicted values of all previous methods with the new sampling results showed that the indirect approach gives more accurate results (Figure-31).

10. ENGINEERING POST-PREDICTION APPLICATIONS

Each geostatistical model identifies some potential risk-prone areas, with the aim of reducing the conceptual model uncertainty and risks in geotechnical design and underground mining operations, each grid point in the study area is given a minimum RMR value based on the previous interpolation maps considering the possible worst scenario (Figure-32):

$$\mathrm{RMR} = \mathrm{Min}\ \{\mathrm{IDW}, \mathrm{OK_i}, \mathrm{OK_d}, \mathrm{OCK_1}, \mathrm{OCK_2}, \mathrm{GCS_D}, \mathrm{GCS_i}\} \quad (18)$$

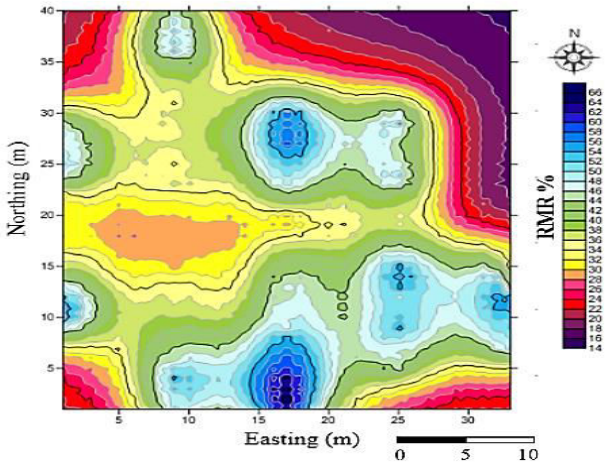

Figure-32. RMR resulting map.

The RMR resulting map can be a useful tool to derive rock mass geomechanical parameters such as uniaxial compressive strength (σ_{cm}) and equivalent young modulus (E_m) that can be used for further numerical simulation and engineering work as if it were an equivalent continuous medium.

When numerical models are used as a tool of mining stability analysis, rock mass strength is defined in terms of a strength envelope that may be the linear case, like Mohr-Coulomb or non-linear like that suggested by Hoek.

10.1 Generalized Hoek-Brown parameters

In most cases, it is not practically possible to carry out triaxial tests on rock masses at a large scale which is necessary to obtain direct values of Generalized Hoek-Brown parameters. The Hoek–Brown criterion relates the strength envelope to the rock mass classification through the Geological strength index (GSI) or RMR indexes and allows strength assessment based on the previous interpolated maps. The Generalized Hoek-Brown criterion parameters (Hoek, Carranza-Torres, Corkum, 2002) [18], are given by the following equations:

$$m_b = m_i . \exp\left(\frac{GSI - 100}{24 - 14D}\right) \quad (19)$$

For $RMR_{76} < 18$ (Hoek, Kaiser, and Bawden, 1995) [19]:

$$GSI = RMR_{76} \quad (20)$$

S and a are constants for the rock mass given by the following relationships:

$$s = \mathrm{Exp}\left(\frac{GSI - 100}{9 - 3D}\right) \quad (21)$$

$$a = \frac{1}{2} + \frac{1}{6}\left(e^{-\frac{GSI}{15}} - e^{-\frac{20}{3}}\right) \quad (22)$$

m_b : Reduced value of the material
m_i : Intact rock constant
GSI : Geological Strength Index
D : Disturbance Factor.

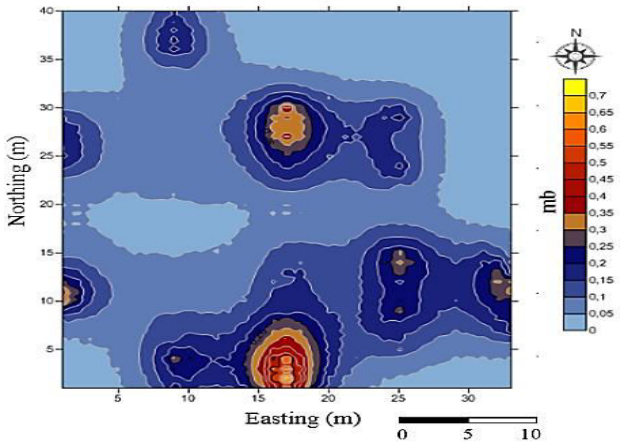

Figure-33. 2D map of mb parameter.

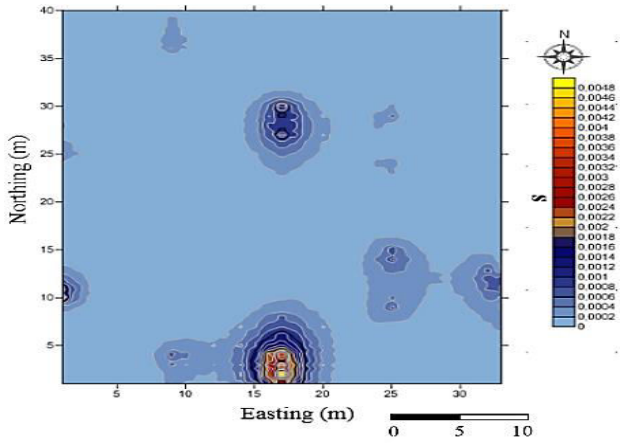

Figure-34. 2D map of s parameter.

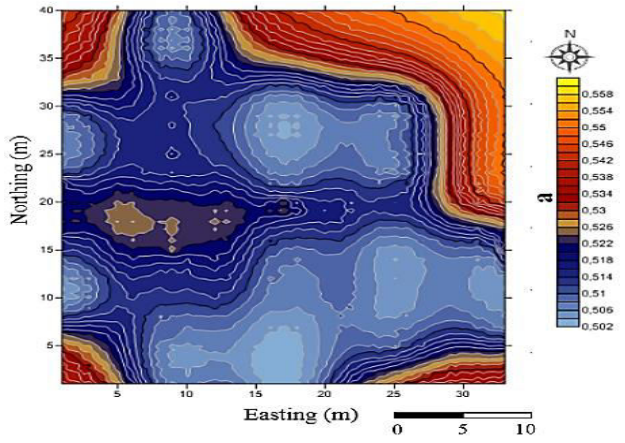

Figure-35. 2D map of a parameter.

The deformation modulus is a required input parameter for different types of numerical analyses; therefore it is necessary to obtain realistic values of rock mass young modulus using the previously calculated parameters.

The generalized equation (Hoek, Diederichs, 2006) [20]:

$$E_m(MPa) = E_i\left(0.02 + \frac{1-\frac{D}{2}}{1+e^{\left(\frac{60+15D-GSI}{11}\right)}}\right) \quad (23)$$

Using the version 2002 of the Hoek-Brown equation, the ratio of the strength of the rock mass and the intact rock is:

$$\sigma_{cm} = s^a \sigma_c \quad (24)$$

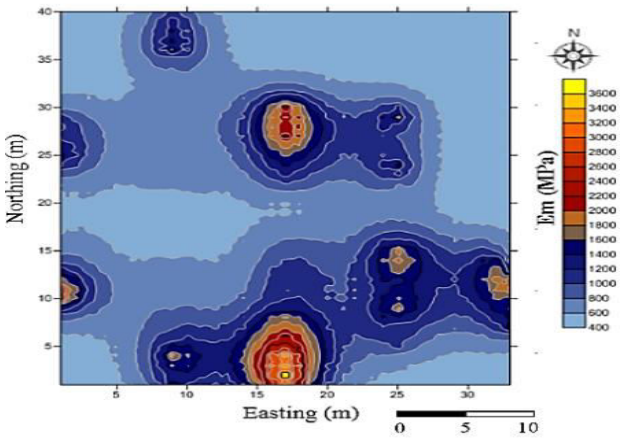

Figure-36. 2D map of rock mass young modulus.

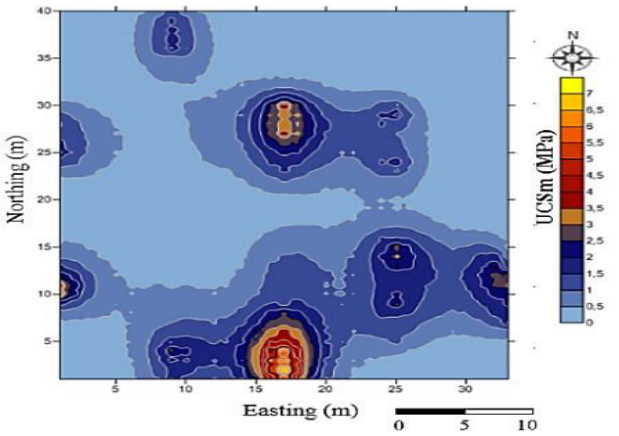

Figure-37. 2D map of rock mass UCS.

10.2 Mohr-coulomb parameters

In case of using the Mohr-Coulomb failure criterion, it is necessary to estimate the cohesion (φ_m) and the friction angle(c_m) parameters of the rock masses which are related to the RMR value according to Bieniawski [21]

Aydan and Kawamoto [22] proposed a linear relationship between the internal friction angle and the RMR value:

$$\varphi_m = 20 + 0.5RMR \quad (25)$$

In this case, the cohesion can be calculated from the friction angle and the rock mass strength by the following equation:

$$c_m = \frac{\sigma_{cm}}{2}\frac{1-sin\varphi_m}{cos\varphi_m} \quad (26)$$

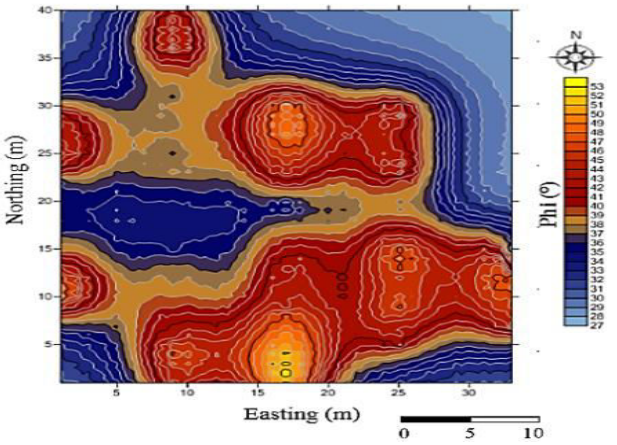

Figure-38. 2D map of rock mass friction angle.

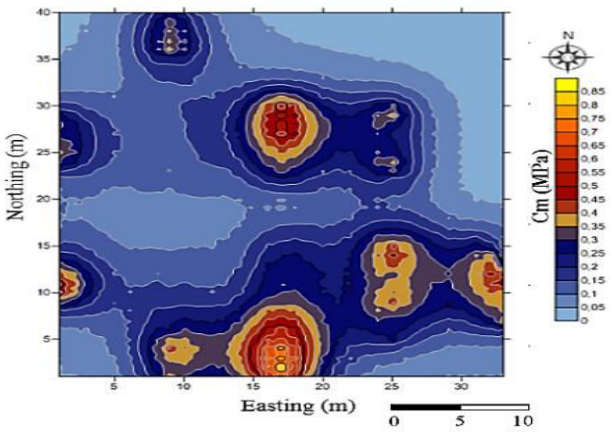

Figure-39. 2D map of rock mass cohesion.

11. CONCLUSIONS

The accurate prediction of geotechnical variables and the risk level is very important for any underground mining project, in this paper, we presented an alternative of traditional approaches, methodologies based on geostatistical estimation and simulation techniques were carried out to determine the expected RMR and its underlying parameters and provides a risk failure analysis with a measure of the uncertainty at any target location.

The proposed indirect estimation and simulation methods outperformed the more frequently used direct approach and shows a more accurate map with low error coefficients which makes them adequate for RMR modeling. However, it should be noted that is high computational and more pre-processing time needed.

This research showed that each geostatistical model identifies potential risk-prone areas in which failures could be experienced, superposing the different resulting maps allowed us to define low-risk conservative RMR model.

The resulting map of the indirect approach allowed taking into account the nonlinear nature, directional behavior of the RMR constitutive parameters which can be used to assist engineers in proposing suitable excavation techniques and an appropriate support system. The developed model help to assess different geomechanical parameters that can use to develop numerical models that explicitly consider the rock mass heterogeneity.

REFERENCES

[1] Ferrari F., Apuani T., Giani G.P. 2014. Rock mass rating spatial estimation by geostatistical analysis. Int J Rock Mech Min Sci. 70, 162-176.

[2] Marisa P., Javier V., Tiago M., Xavier E. 2016. Geostatistical simulation to map the spatial heterogeneity of geomechanical parameters: A case study with rock mass rating. Engineering Geology. 205, 93-103.

[3] Hesameddin E., Kamran E., Raynald J. 2017. Modelling Geomechanical Heterogeneity of Rock Masses Using Direct and Indirect Geostatistical Conditional Simulation Methods. Rock Mech Rock Eng. 50, 3175-3195.

[4] Bieniawski Z.T. 1993. Classification of Rock Masses for Engineering: The RMR System and Future Trends. Comprehensive rock engineering. 3, 522-542.

[5] Burrough P.A., McDonnell R.A. 1998. Principles of Geographical Information Systems. Oxford University Press Inc., New York. pp. 32-333.

[6] Journel A.G., Huijbregts C.J. 1978. Mining Geostatistics. Academic Press, London. Karacan,

[7] Isaaks E.H., Srivastava R. 1989. An Introduction to Applied Geostatistics. Oxford University Press, New York. 561.

[8] Goovaerts P. 1997. Geostatistics for Natural Resources Evaluation. Oxford University Press, New York.

[9] Dowd P.A. 1993. Geostatistical simulation, course notes for the MSc. in Mineral Resource and Environmental Geostatistics, University of Leeds. 123.

[10] Robertson G.P. 1987. Geostatistics in ecology: Interpolating with known variance. Ecology. 68-3, 744-748.

[11] Cambardella C.A. 1994. Field-scale variability of soil properties in central Iowa soils. Soil Science Society of America Journal. 58, 1501-1511.

[12] Deutsch C.V. and A.G. Journel. 1992. Geostatistical software library and user's guide. Oxford University Press, New York. p. 340.

[13] Yates S.R., Warrick A.W. 1987. Estimating soil water content using cokriging. Soil Sci. Soc. Am. J. 51, 23-30.

[14] Templeton, Gary F. 2011. A Two-Step Approach for Transforming Continuous Variables to Normal: Implications and Recommendations for IS Research," Communications of the Association for Information Systems. 28(Article 4).

[15] Webster R., Oliver M. 2001. Geostatistics for Environmental Scientists. John Wiley & Sons, Ltd, Chichester.

[16] Kravchenko A., Bullock D. G. 1999. A comparative study of interpolation methods for mapping soil properties. Agron J. 91, 393-400.

[17] Olea R.A. 1999. Geostatistics for Engineers and Earth Scientists. Kluwer Academic Publishers. 303.

[18] Carranza-Torres C.T., Corkum, B.T. 2002. Hoek-Brown failure criterion: 2002 edition. In Hammah, Bawden, Curran &Telesnicki (eds.), Proc. of the 5th North American Rock Mech. Symp. Toronto, 7-10 July. University of Toronto Press. 267-274

[19] Hoek, E., Kaiser, P.K. and Bawden, W.F. 1995. Support of Underground Excavations in Hard Rock. AA Balkema, Rotterdam.

[20] Hoek E., Diederichs M.S. 2006. Empirical estimation of rock mass modulus. International Journal of Rock Mechanics and Mining Sciences. 43, 203-215.

[21] Bieniawski Z.T. 1989. Engineering Rock Mass Classifications. 272.

[22] Aydan Ö., Kawamoto T. 2001. The stability assessment of a large underground opening at great depth. In: Proceedings of the 17th International Mining Congress., Turkey, Ankara. 277-288.